arXiv:1611.08604v1 [hep-th] 25 Nov 2016

Schwinger-type parametrization of open string worldsheets

Sam Playle*, Stefano Sciuto

Dipartimento di Fisica, Università di Torino
and INFN, Sezione di Torino
Via P. Giuria 1, I-10125 Torino, Italy

Abstract

A parametrization of (super) moduli space near the corners corresponding to bosonic or Neveu-Schwarz open string degenerations is introduced for worldsheets of arbitrary topology. With this parametrization, Feynman graph polynomials arise as the $\alpha' \to 0$ limit of objects on moduli space. Furthermore, the integration measures of string theory take on a very simple and elegant form.

Keywords: Schottky groups, strings, superstrings, wordline formalism, supermaniforlds

1. Introduction

A very useful parametrization of the moduli of multiloop Riemann surfaces is given by Schottky groups, which manifested themselves automatically in the earliest approaches to multiloop string amplitudes. In this letter we describe (in section 2) a scheme for co-ordinatizing the moduli space of orientable *open string* worldsheets, in which all $3g-3+n$ real moduli are realized as 'lengths' of plumbing fixtures. In section 3 we see how Feynman graphs with various distinct topologies arise as the $\alpha' \to 0$ limit of such worldsheets, given an appropriate mapping between dimensionless pinching parameters p_i and Schwinger parameters t_i. In section 4 we show how the construction can be extended to the Neveu-Schwarz sector of superstrings, and present the elegant form taken by the leading part of the string measure in the pinching moduli. The pinching moduli are 'canonical parameters' in the sense of section 6.3 of reference [1], so their use makes Berezin integration on supermoduli

*Corresponding author
Email addresses: playle@to.infn.it (Sam Playle), sciuto@to.infn.it (Stefano Sciuto)

space unambiguous. Proofs omitted in this letter are to be provided in a forthcoming work [2].

2. The parametrization

We are interested in describing worldsheets near complete "open string" degenerations; in such regions of moduli space the worldsheets may be constructed from 3-punctured discs glued together with strips. The topologically distinct degenerations can be classified as cubic ribbon graphs (*i.e.* graphs with a fixed cyclic ordering of the three edges incident on each vertex). Given a (not necessarily planar) cubic ribbon graph, we want to find "pinching parameters" $\{p_i\}$, *i.e.* local coordinates on Schottky space such that taking $p_i \to 0$ gives the corner corresponding to that degeneration.

To achieve this, we will provide an algorithm for writing down the g Schottky group generators γ_i and the n positions of punctures x_j as functions of the pinching parameters for a given cubic ribbon graph.

The algorithm may be arrived at by considering transition functions on a surface obtained by gluing together 3-punctured discs with open-string plumbing fixtures. All transition functions will be composed of two fundamental ones: one that cycles between local coordinates around the three punctures on a disc, and one which moves from one end of a plumbing fixture to the other.

Let us consider first of all a 3-punctured disc. Let the punctures be labelled a_1, a_2 and a_3 with a clockwise ordering. We will need three local coordinate charts z_1, z_2, z_3 which vanish at their respective punctures; $z_i(a_i) = 0$. The upper-half-plane is the image of the disc under z_i and its boundary is mapped onto the projective real line. Let us also specify

$$z_i(a_{i+1}) = \infty \ ; \qquad\qquad z_i(a_{i-1}) = 1 \ , \tag{1}$$

where the indices are mod 3. Then there is a unique Möbius map ρ which acts as a **transition function cycling the three charts**. We want to have $z_i = \rho(z_{i+1})$, then we need

$$\rho(0) = \infty \ ; \qquad\qquad \rho(\infty) = 1 \ ; \qquad\qquad \rho(1) = 0 \ . \tag{2}$$

This is given by $\rho(z) = 1 - 1/z$, or as a matrix acting on the homogeneous coordinates,

$$\rho = \begin{pmatrix} 1 & -1 \\ 1 & 0 \end{pmatrix} \ . \tag{3}$$

which, of course, satisfies $\rho^3 = \mathrm{Id}$. So in general, on a 3-punctured disc the transition functions between these canonical charts are given by

$$\begin{cases} \rho & \leftrightarrow \text{move anticlockwise around the disc} \\ \rho^{-1} & \leftrightarrow \text{move clockwise around the disc.} \end{cases} \tag{4}$$

The other ingredient is the **open string plumbing fixture**. Suppose our surface includes two charts z, w whose images are contained in the upper-half-plane and include semi-discs of radius 1 centred on 0. Then if we fix a "pinching parameter" p with $0 < p < 1$ and cut out the semi-discs $|z| < p$, $|w| < p$ we can impose the equation

$$z\, w = -p \ , \tag{5}$$

for $|z| < 1$, $|w| < 1$, which we call an open string plumbing fixture between the two charts. Topologically, the effect is to attach a strip to the boundary of the surface, either adding a 'handle' or joining two previously disconnected components. When we take $p \to 0$ the strip degenerates leaving a node joining $z^{-1}(0)$ to $w^{-1}(0)$.

We can view the plumbing fixture as a transition function from the chart at one end to the chart at the other: let us define a Möbius map σ_p such that Eq. (5) can be written as $w = \sigma_p(z)$, *i.e.* $\sigma_p(z) \equiv -p/z$, or as a matrix

$$\sigma_p = \frac{1}{\sqrt{p}} \begin{pmatrix} 0 & -p \\ 1 & 0 \end{pmatrix} \ . \tag{6}$$

We can summarize its use as

$$\sigma_p \leftrightarrow \text{ traverse a plumbing fixture with pinching parameter } p \ . \tag{7}$$

Now let us consider a cubic ribbon graph Γ. Let us assign *three* coordinate charts to each vertex, with one associated to each incident half-edge. We can write down a sequence composed of the following two moves taking us from one chart to any other one:

- Moving (anti)clockwise between two charts associated to different half-edges incident at the same vertex.
- Moving from a chart associated to a half-edge of an internal edge E_k to a chart associated to its half-edge at the vertex at the other end.

It's crucial that an internal edge not be traversed before first moving onto the chart associated to its half-edge.

A sequence of such moves can be translated into a transition function with the following dictionary:

$$\begin{cases} \text{move anticlockwise around a vertex} & \leftrightarrow \rho \\ \text{move clockwise around a vertex} & \leftrightarrow \rho^{-1} \\ \text{traverse } E_k & \leftrightarrow \sigma_{p_k} \equiv \sigma_k \,, \end{cases} \tag{8}$$

where we have associated a pinching parameter p_k to every internal edge E_k.

Note that for multiply-connected graphs, this procedure gives multiple, distinct transition functions from one chart to another, since there are multiple paths between each pair of charts and each path gives a different transition function. This is because there is a Schottky group: each transition function is well-defined modulo the group action.

To be more explicit, let us pick a **"base chart"** z (*i.e.* a choice of one of the vertices in Γ *and* one of its incident half-edges). If the surface has g loops, then we can find g homologically independent closed paths P_i starting and ending at z. For each closed path, we can use Eq. (8) to write down a Möbius map; these g Möbius maps are the Schottky group generators γ_i.

Furthermore, suppose Γ has n external edges (corresponding to punctures in the surface). Each external edge has a coordinate chart, in which the punctures are at 0. We can write down paths P_j from these charts back to the base chart z, and again using the dictionary Eq. (8), we can find Möbius maps V_j which are transition functions from these charts to the base chart z. Then the positions of the punctures as seen in the base chart will be given as

$$x_j = V_j(0) \,. \tag{9}$$

So we have defined a Riemann surface by a set of transition functions which depend on a set of parameters $\{p_i\}$. The number of parameters equals the number of internal edges, which by elementary graph topology is $3g-3+n$, coinciding with the real dimension of open string Schottky space. The canonical Schottky coordinates (multipliers, fixed points and puncture coordinates) can be expressed in terms of the p_i's, so these provide a new set of coordinates for Schottky space. Moreoever, in the limit $p_i \to 0$, the surface totally degenerates into a collection of 3-punctured discs joined together at nodes, with the topology corresponding to the graph Γ used to define the p_i's.

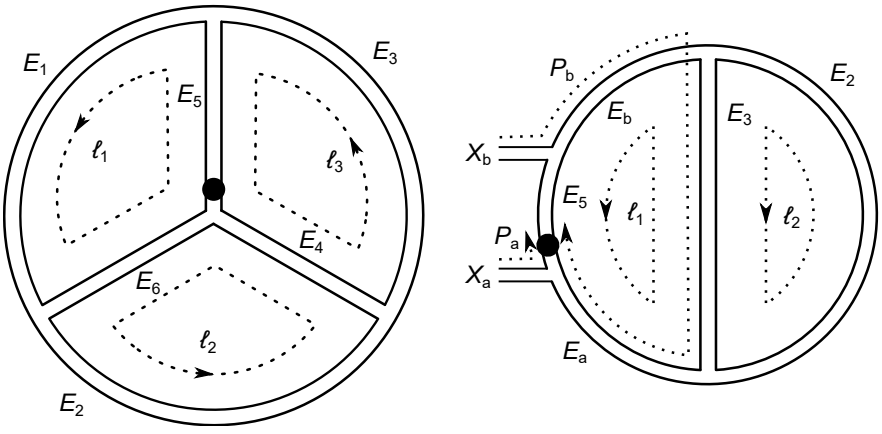

Figure 1: Two cubic ribbon graphs. Internal edges are labelled by E_i and external edges are labelled with X_j. The big dots indicate the chosen base charts. Dotted lines indicate paths: loops are labelled ℓ_k while paths from X_j to the base chart are labelled P_j.

Use of these pinching parameters as integration variables on moduli space gives the bosonic string measure an elegant and simple form which we describe at the end of section 4.1, since it is similar to the analogous expression for the NS sector of superstrings [2].

2.1. An example at 3-loop

Let us consider the 3-loop "Mercedes-Benz" diagram shown in Fig. 1a. We can write down the Schottky group for this graph according to the procedure in section 2. The big dot indicates a choice of coordinate chart to use as our base chart. A basis of three loops ℓ_1, ℓ_2, ℓ_3 is indicated. For each of these loops, we can write down a sequence of the basic 'moves' needed to go around the loop and arrive back in the base chart, as follows (reading right-to-left):

$$\ell_1 = \text{CW} \cdot E_6 \cdot \text{CW} \cdot E_1 \cdot \text{CW} \cdot E_5 \tag{10}$$

$$\ell_2 = \text{ACW} \cdot E_4 \cdot \text{CW} \cdot E_2 \cdot \text{CW} \cdot E_6 \cdot \text{ACW} \tag{11}$$

$$\ell_3 = E_5 \cdot \text{CW} \cdot E_3 \cdot \text{CW} \cdot E_4 \cdot \text{CW}\,, \tag{12}$$

where (A)CW means "move to the chart that is (anti)clockwise from the current one on the same vertex" and E_i means "move to the chart at the other end of the

edge E_i". Then the dictionary Eq. (8) gives us the following matrices as the three Schottky generators:

$$\gamma_1 = \rho^{-1}\,\sigma_6\,\rho^{-1}\,\sigma_1\,\rho^{-1}\,\sigma_5 = \frac{1}{\sqrt{k_1}}\begin{pmatrix} 1 & 0 \\ 1+p_6(1+p_1) & k_1 \end{pmatrix} \tag{13}$$

$$\gamma_2 = \rho\,\sigma_4\,\rho^{-1}\,\sigma_2\,\rho^{-1}\,\sigma_6\,\rho = \frac{-1}{\sqrt{k_2}}\begin{pmatrix} 1+p_4(1+p_2(1+p_6)) & -1-p_4(1+p_2) \\ p_4(1+p_2(1+p_6)) & -p_4(1+p_2) \end{pmatrix} \tag{14}$$

$$\gamma_3 = \sigma_5\,\rho^{-1}\,\sigma_3\,\rho^{-1}\,\sigma_4\,\rho^{-1} = \frac{1}{\sqrt{k_3}}\begin{pmatrix} k_3 & -p_5(1+p_3(1+p_4)) \\ 0 & 1 \end{pmatrix} \tag{15}$$

where the multipliers k_i are

$$k_1 = p_1\,p_5\,p_6 \qquad\qquad k_2 = p_2\,p_4\,p_6 \qquad\qquad k_3 = p_3\,p_4\,p_5\,, \tag{16}$$

i.e. simply the products of the pinching parameters of the edges in the respective loops (this is true in general whenever a loop ℓ_i is conjugate to one whose turns are either all CW or all ACW). The attractive and repulsive Schottky fixed points, u_i and v_i respectively, can be computed as

$$u_1 = 0 \qquad v_1 = \infty \qquad v_2 = 1 \qquad v_3 = \frac{1+p_6(1+p_1)}{p_6(1+p_1(1+p_5))} \tag{17}$$

$$u_2 = \frac{1+p_6((1+p_4+p_1(1+p_4(1+p_2)(1+p_5)))+p_1\,p_2\,p_4\,p_5\,p_6)}{p_6(1+p_4(1+p_2))(1+p_1(1+p_5))} \tag{18}$$

and

$$u_3 = \frac{1+p_5((1+p_6+p_3(1+p_6(1+p_1)(1+p_4)))+p_1\,p_3\,p_4\,p_5\,p_6)}{p_5\,p_6(1+p_3(1+p_4))(1+p_1(1+p_5))}\,. \tag{19}$$

2.2. An example with external edges

For a second example, let us consider the $g = 2$, $n = 2$ graph in Fig. 1b. The two loops may be written as

$$\ell_1 = E_5 \cdot \text{CW} \cdot E_b \cdot \text{CW} \cdot E_3 \cdot \text{CW} \cdot E_a \cdot \text{CW} \tag{20}$$

$$\ell_2 = \text{ACW} \cdot E_a \cdot \text{ACW} \cdot E_3 \cdot \text{CW} \cdot E_2 \cdot \text{ACW} \cdot E_a \cdot \text{CW} \tag{21}$$

so the Schottky group generators are

$$\gamma_1 = \sigma_5\,\rho^{-1}\,\sigma_b\,\rho^{-1}\,\sigma_3\,\rho^{-1}\,\sigma_a\,\rho^{-1} \tag{22}$$

$$\gamma_2 = (\rho\,\sigma_a\,\rho)\,\sigma_3\,\rho^{-1}\,\sigma_2\,\rho^{-1}\,(\rho\,\sigma_a\,\rho)^{-1}\,, \tag{23}$$

whose fixed points and multipliers may be computed straightforwardly. The paths P_i from the external edges X_i to the base chart may be written as

$$P_a = \text{CW} \qquad\qquad P_b = \text{ACW} \cdot E_a \cdot \text{ACW} \cdot E_3 \cdot \text{ACW} \cdot E_b \cdot \text{CW} \tag{24}$$

so

$$V_a = \rho^{-1} \qquad\qquad V_b = \rho\,\sigma_a\,\rho\,\sigma_3\,\rho\,\sigma_b\,\rho^{-1} \tag{25}$$

hence the coordinates of the punctures in the base chart are

$$x_a = V_a(0) = 1\,, \qquad\qquad x_b = V_b(0) = \frac{1 + p_b(1 + p_3(1 + p_a))}{p_a\,p_b\,p_3}\,. \tag{26}$$

3. The field theory limit

Suppose a cubic ribbon graph Γ is used to parametrize a Schottky group according to the procedure in section 2. Let us hypothesize the following expression for the $3g - 3 + n$ pinching parameters p_i in terms of Schwinger parameters t_i (where α' is the Regge slope):

$$p_i = \mathrm{e}^{-t_i/\alpha'}\,. \tag{27}$$

With this, we can study the $\alpha' \to 0$ asymptotics of various objects defined in terms of the open string worldsheets. We find that the limiting behaviour is given in terms of purely graph-theoretic objects defined in terms of Γ, where the t_i are taken as Schwinger parameters for the corresponding internal edges E_i.

3.1. Period matrix

The period matrix of a Riemann surface given by a Schottky group (with a compatible marking) is equal to the following series [3]

$$\tau_{ij} = \frac{1}{2\pi\mathrm{i}}\Big(\delta_{ij}\,\log k_i \;-\; {}^{(i)}{\sum_{\gamma_\alpha}}'{}^{(j)}\,\log\frac{u_i - \gamma_\alpha(v_j)}{u_i - \gamma_\alpha(u_j)}\frac{v_i - \gamma_\alpha(u_j)}{v_i - \gamma_\alpha(v_j)}\Big) \tag{28}$$

where the summation is over all Schottky group elements γ_α whose left-most factor is not $\gamma_i^{\pm n}$ and whose right-most factor is not $\gamma_j^{\pm n}$. We can compute this, for example,

for the 3-loop worldsheet described in section 2.1. We find

$$\tau_{ij} = \frac{1}{2\pi \mathrm{i}} \begin{pmatrix} \log p_1 p_5 p_6 & -\log p_6 & -\log p_5 \\ -\log p_6 & \log p_2 p_4 p_6 & -\log p_4 \\ -\log p_5 & -\log p_4 & \log p_3 p_4 p_5 \end{pmatrix} + \mathcal{O}(p_i)\,. \tag{29}$$

All Schotty group elements other than the identity give an $\mathcal{O}(p_i)$ contribution in Eq. (29).

We can also compute the *graph period matrix* for a g-loop graph Γ with a basis $\{\ell_i\}$ of loops. This is given by [4]

$$\theta_{ij} = \sum_k \langle \ell_i, \ell_j \rangle^k \, t_k \,, \tag{30}$$

where for paths P_1, P_2 we define

$$\langle P_1, P_2 \rangle^k \equiv \begin{cases} 1 & \text{if } P_1 \text{ and } P_2 \text{ cross } E_k \text{ in the same direction} \\ -1 & \text{if } P_1 \text{ and } P_2 \text{ cross } E_k \text{ in opposite directions} \\ 0 & \text{if } P_1 \text{ and } P_2 \text{ do not both cross } E_k. \end{cases} \tag{31}$$

The graph period matrix for the graph in Fig. 1a is given by

$$\theta_{ij} = \begin{pmatrix} t_1 + t_5 + t_6 & -t_6 & -t_5 \\ -t_6 & t_2 + t_4 + t_6 & -t_4 \\ -t_5 & -t_4 & t_3 + t_4 + t_5 \end{pmatrix} . \tag{32}$$

Clearly, with the use of Eq. (27) the matrices in Eq. (29) and Eq. (32) satisfy

$$\mathrm{i}\,\theta_{ij} = \lim_{\alpha' \to 0} 2\pi\alpha' \tau_{ij} \,. \tag{33}$$

In fact, Eq. (33) is true in general as a relation between an arbitrary g-loop, n-point cubic graph Γ and the surface parametrized with it as in section 2 [2].

The determinant of a graph's period matrix is the graph's first Symanzik polynomial, which appears in the denominator of the corresponding Feynman integrals [5]. Eq. (33) elucidates how this can arise from the powers of $\det(2\pi \,\mathrm{Im}\,\tau)$ which appear in the denominator of the string measure on moduli space.

3.2. Green's function

This parametrization also allows us to see how the worldline Green's function can arise as the $\alpha' \to 0$ limit of the worldsheet Green's function.

We use the results of [4], where it is shown that the worldline Green's function between two external edges X_1, X_2 on a g-loop graph Γ with a basis $\{\ell_i\}$ of loops may be written as

$$G_{X_1X_2} = -\frac{1}{2}s + \frac{1}{2}\,\vec{v}\cdot\theta^{-1}\cdot\vec{v}\,. \tag{34}$$

where we've picked some path P from X_1 to X_2 and then in terms of Eq. (31),

$$s \equiv \langle P, P\rangle \qquad\qquad v_i \equiv \langle \ell_i, P\rangle\,. \tag{35}$$

G can be found from the $\alpha' \to 0$ limit of

$$\widehat{\mathcal{G}}(x_1,x_2) \equiv \mathcal{G}(x_1,x_2) - \frac{1}{2}\log(V_1'(0)V_2'(0)) \tag{36}$$

where V_i is the transition function that goes from the chart associated with the external edge X_i to the base chart z, and $x_i = V_i(0)$ is the z coordinate of the puncture. $\mathcal{G}(w,z)$ is the worldsheet Green's function given by [6]

$$\mathcal{G}(z,w) = \log E(z,w) - \frac{1}{2}\Big(\int_z^w \vec{\omega}\Big)\cdot(2\pi\mathrm{Im}\,\tau)^{-1}\cdot\Big(\int_z^w \vec{\omega}\Big)\,. \tag{37}$$

Here $E(z,w)$ is the Schottky-Klein prime form

$$E(z,w) = (z-w)\prod_\alpha{}' \frac{z-\gamma_\alpha(w)}{z-\gamma_\alpha(z)}\frac{w-\gamma_\alpha(z)}{w-\gamma_\alpha(w)} \tag{38}$$

where the Schottky group product includes one from each pair of inverse elements $\{\gamma_\alpha, \gamma_\alpha^{-1}\}$. ω_i are the Abelian differentials, given by

$$\omega_i(z) = \sum_\alpha{}^{(i)}\Big(\frac{1}{z-\gamma_\alpha(u_i)} - \frac{1}{z-\gamma_\alpha(v_i)}\Big)\,\mathrm{d}z \tag{39}$$

where the sum is over all Schottky group elements whose right-most factor is not $\gamma_i^{\pm n}$. We find that

$$\frac{1}{2}\,s = \lim_{\alpha'\to 0}\alpha'\log\frac{E(x_1,x_2)}{\sqrt{V_1'(0)V_2'(0)}} \qquad\qquad v_i = -\lim_{\alpha'\to 0}\alpha'\int_{x_1}^{x_2}\omega_i \tag{40}$$

which along with Eq. (33) gives

$$G_{X_1X_2} = -\lim_{\alpha'\to 0} \alpha' \, \widehat{\mathcal{G}}(x_1, x_2)\,. \tag{41}$$

As an example, consider the $g = 2$, $n = 2$ graph in Fig. 1b, whose corresponding pinching parametrization was worked out in section 2.2.

Let us choose the path P between the two external edges to be given in terms of Eq. (24) by $P = P_b^{-1} \cdot P_a$; using Eq. (35) this gives

$$s = t_a + t_b + t_3 \qquad\qquad \vec{v} = (t_a + t_b + t_3\,,\, -t_3)^{\mathrm{t}}\,. \tag{42}$$

From the Schottky group formulae, we can use

$$V_a'(0) = 1\,, \qquad\qquad V_b'(0) = \frac{1}{p_a\, p_b\, p_3}\,. \tag{43}$$

to find

$$\log \frac{E(x_b, x_a)}{\sqrt{V_a'(0) V_b'(0)}} = \log \frac{x_b - x_a}{\sqrt{V_a'(0) V_b'(0)}} + \mathcal{O}(p_i) = -\frac{1}{2} \log(p_a\, p_b\, p_3) + \mathcal{O}(p_i)\,, \tag{44}$$

which converges to $s/2\alpha'$ after using Eq. (27) and taking $\alpha' \to 0$. Similarly, we can compute $\int_{x_a}^{x_b} \omega_i$. The only Schottky group element which contributes at leading order is the identity; we find

$$\int_{x_b}^{x_a} \vec{\omega}(z) = \Big[\log \frac{z - u_i}{z - v_i} \Big]_{x_b}^{x_a} + \mathcal{O}(p_j) = \big(-\log(p_a\, p_b\, p_3)\,,\, \log(p_3) \big)^{\mathrm{t}} + \mathcal{O}(p_j)\,; \tag{45}$$

again, this asymptotes to $\vec{v}/\alpha'$ in the limit $\alpha' \to 0$. Thus, combining Eq. (45) and Eq. (44) and computing the period matrix as in section 3.1, we find that for the surface parametrized by the graph in Fig. 1b,

$$\lim_{\alpha'\to 0} \alpha' \widehat{\mathcal{G}}(x_b, x_a) = \frac{t_5}{2} - \frac{t_5^2 (t_2 + t_3)}{2 \det \theta} = -G\,. \tag{46}$$

This holds in general. Since Feynman integrals for Φ^3 scalar QFTs can be written down using only the worldline Green's function [7], this clarifies how the Feynman diagrams arise from the various corners of moduli space in the corresponding string theory.

4. Superstrings

The construction in section 2 can be adapted for the Neveu-Schwarz (NS) sector of superstrings in the RNS formalism, in which the worldsheets are taken as super Riemann surfaces (SRS) [1]. We use the formalism of super Schottky groups [8, 9] following the notation of section 2.2 of [10].

A number of modifications must be made to the construction in section 2. Firstly, the 3-punctured discs must be replaced by SRS discs with three NS punctures (NNN discs). While 3-punctured discs have no moduli, NNN discs have one Grassmann-odd supermodulus. If the punctures are at $\boldsymbol{a}_1$, $\boldsymbol{a}_2$, $\boldsymbol{a}_3$ and $\boldsymbol{z} = z|\zeta$ is a global superconformal coordinate, then

$$\Theta_{\boldsymbol{a}_1\boldsymbol{a}_2\boldsymbol{a}_3} \equiv \pm\frac{\zeta_1(\boldsymbol{z}_2 \dot{-} \boldsymbol{z}_3) + \zeta_2(\boldsymbol{z}_3 \dot{-} \boldsymbol{z}_1) + \zeta_3(\boldsymbol{z}_1 \dot{-} \boldsymbol{z}_2) + \zeta_1\zeta_2\zeta_3}{\sqrt{(\boldsymbol{z}_1 \dot{-} \boldsymbol{z}_2)(\boldsymbol{z}_2 \dot{-} \boldsymbol{z}_3)(\boldsymbol{z}_3 \dot{-} \boldsymbol{z}_1)}} \tag{47}$$

is a superprojective (pseudo)invariant, and a modulus of an NNN disc. Here $\boldsymbol{z}_i \equiv \boldsymbol{z}(\boldsymbol{a}_i)$ and $\boldsymbol{z}_i \dot{-} \boldsymbol{z}_j \equiv z_i - z_j - \zeta_i\zeta_j$. To account for this, we attach an odd parameter Θ_i to every vertex V_i in our cubic ribbon graph Γ. Whereas in the bosonic construction a single matrix ρ is used to 'rotate' around any vertex, now each vertex V_i must get its own separate matrix $\boldsymbol{\rho}_{\Theta_i}$. It is given by the OSp(1|2) matrix

$$\boldsymbol{\rho}_\Theta \equiv \left(\begin{array}{cc|c} -1 & 1 & -\Theta \\ -1 & 0 & 0 \\ \hline -\Theta & 0 & 1 \end{array}\right) \tag{48}$$

which permutes the points with homogenous coordinates $(0, 1|0)^{\mathrm{t}}$, $(1, 0|0)^{\mathrm{t}}$, $(1, 1|\Theta)^{\mathrm{t}}$.

The second modification to the construction in section 2 is that the internal edges of the cubic ribbon graph Γ must be given orientations, *i.e.* Γ must be a *directed* cubic ribbon graph. The reason for this is that the NS plumbing fixture is asymmetric unlike its bosonic equivalent. If $\boldsymbol{z} = z|\zeta$ and $\boldsymbol{w} = w|\psi$ are two superconformal charts at opposite ends of an NS plumbing fixture, then they satisfy

$$z\,w = -\varepsilon^2\,, \qquad z\,\psi = \varepsilon\,\zeta\,, \qquad w\,\zeta = -\varepsilon\,\psi\,, \qquad \psi\,\zeta = 0\,, \tag{49}$$

where we call ε the "NS pinching parameter". Eq. (49) is not symmetric under swapping $\boldsymbol{z} \leftrightarrow \boldsymbol{w}$ without also swapping $\varepsilon \leftrightarrow -\varepsilon$. We can rewrite Eq. (49) in terms of a transition function as $\boldsymbol{w} = \boldsymbol{\sigma}_\varepsilon(\boldsymbol{z})$, where $\boldsymbol{\sigma}_\varepsilon(\boldsymbol{z}) \equiv -\varepsilon^2/z \,\big|\, \varepsilon\,\zeta/z$, or as an

OSp(1|2) matrix,

$$\boldsymbol{\sigma}_\varepsilon \equiv \left(\begin{array}{cc|c} 0 & -\varepsilon & 0 \\ \varepsilon^{-1} & 0 & 0 \\ \hline 0 & 0 & 1 \end{array}\right) . \tag{50}$$

The general idea of the approach to writing down a super-Schottky group from a directed cubic ribbon graph Γ is the same as in the bosonic case. Each cubic vertex in Γ has three associated superconformal charts (one for each incident half-edge). Let us pick one as a 'base chart' $\boldsymbol{z}$. If Γ is a g loop graph, we can find g independent closed paths starting at the base chart. After decomposing each path ℓ_i into the same set of basic 'moves' as in the bosonic case, we can translate it into a super Schottky group generator $\boldsymbol{\gamma}_i$ using the following dictionary:

$$\begin{cases} \text{move anticlockwise around the vertex } V_i & \leftrightarrow \boldsymbol{\rho}_{\Theta_i} \\ \text{move clockwise around the vertex } V_i & \leftrightarrow \boldsymbol{\rho}_{\Theta_i}^{-1} \\ \text{traverse } E_k \text{ in the marked direction} & \leftrightarrow \boldsymbol{\sigma}_{\varepsilon_k} \\ \text{traverse } E_k \text{ against the marked direction} & \leftrightarrow \boldsymbol{\sigma}_{\varepsilon_k}^{-1} . \end{cases} \tag{51}$$

Similarly, for each external edge X_i in Γ, we find a path P_i going from X_i to the base chart and then use the dictionary Eq. (51) to translate P_i into a transition function $\boldsymbol{V}_i$; the $\boldsymbol{z}$ coordinates of the corresponding NS puncture are $x_i|\xi_i = \boldsymbol{V}_i(0|0)$.

A g-loop cubic graph Γ with n external edges has $|V| = 2g-2+n$ cubic vertices and $|E| = 3g-3+n$ internal edges; since we associate a Grassmann odd parameter Θ_i to each vertex V_i and a Grassmann-even parameter ε_k to each edge E_k, we see that we match the dimension of supermoduli space, $\dim(\mathfrak{M}_{g,n}) = 3g-3+n|2g-2+n$. For planar vacuum graphs with $n=0$ which have $|F| = g+1$ faces, we can use the supermoduli space dimension to check Euler's graph formula $|V|-|E|+|F| = 2$.

Note that the parametrization chosen for $g=2$, $n=0$ in references [11, 12] arises as a special case of the procedure described in this section. In those works, it was used to find the $\alpha' \to 0$ limit of the NS superstring amplitude, correctly yielding the sum of 2-loop vacuum Feynman diagrams for the bosonic sector of $\mathcal{N}=4$ SYM in a particular gauge. While the *ad hoc* manipulation described in section 5 of [11] was necessary to correctly choose which even supermoduli to fix before evaluating Berezin integrals (see section 3.4.1 of [13] for why this is important), and to rescale odd supermoduli to symmetrize the factors in the measure, the procedure described here prescribes the same outcome without ambiguity.

4.1. The superstring measure

The super Schottky group expression for the g-loop, n-point superstring measure in the NS sector is given by Eqs. (30) and (31) of [14]. The leading holomorphic part (having dropped the period matrix determinants and nonzero mode parts of the functional determinants) is given in terms of canonical super Schottky variables by

$$[\mathrm{d}\boldsymbol{m}_0]_g^n \equiv \frac{1}{\mathrm{d}\boldsymbol{V}_{abc}} \prod_{i=1}^{n} \frac{\mathrm{d}\boldsymbol{x}_i}{(D\boldsymbol{V}_i^\zeta)(0|0)} \prod_{j=1}^{g} \frac{\mathrm{d}\boldsymbol{u}_i\,\mathrm{d}\boldsymbol{v}_j\,\mathrm{d}q_j}{\boldsymbol{u}_j \dot{-} \boldsymbol{v}_j} \frac{(1+q_j)^2}{q_j^2}\,, \tag{52}$$

and takes a simple and elegant form in terms of these pinching parameters. In Eq. (52) $\boldsymbol{u}_i$ and $\boldsymbol{v}_i$ are the attractive and repulsive fixed superpoints of $\boldsymbol{\gamma}_i$ and q_i is its semimultiplier ($\boldsymbol{\gamma}_i$ is conjugate to $\boldsymbol{z} \mapsto q_i^2 z | q_i \zeta$). $\boldsymbol{x}_i = \boldsymbol{V}_i(0|0)$ is the position of the NS puncture associated to X_i, $\boldsymbol{V}_i^\zeta$ is the odd part of $\boldsymbol{V}_i$ and D is the superderivative. The superprojective volume element is given by

$$\frac{1}{\mathrm{d}\boldsymbol{V}_{abc}} = \frac{\sqrt{(\boldsymbol{a} \dot{-} \boldsymbol{b})(\boldsymbol{b} \dot{-} \boldsymbol{c})(\boldsymbol{c} \dot{-} \boldsymbol{a})}}{\mathrm{d}\boldsymbol{a}\,\mathrm{d}\boldsymbol{b}\,\mathrm{d}\boldsymbol{c}}\,\mathrm{d}\Theta_{\boldsymbol{abc}}, \tag{53}$$

where $\boldsymbol{a}$, $\boldsymbol{b}$ and $\boldsymbol{c}$ are three superpoints chosen from among the $\boldsymbol{x}_i$, $\boldsymbol{u}_j$ and $\boldsymbol{v}_j$ to be gauge-fixed.

Expressed in terms of the pinching supermoduli, Eq. (52) takes on the following very simple form:

$$[\mathrm{d}\boldsymbol{m}_0]_g^n \propto \prod_{V_i} \mathrm{d}\Theta_i \prod_{E_j} \frac{\mathrm{d}\varepsilon_j}{\varepsilon_j^2} \prod_{B} (1+q_B)\,. \tag{54}$$

Here the product runs over all *closed boundaries* B of the ribbon graph Γ, meaning all closed paths in the graph whose decomposition involves either only CW or only ACW turns at the vertices. q_B is the semimultiplier of the super Schottky group element $\boldsymbol{\gamma}_B$ homologous to the path B, which is equal (modulo a sign) to the product of the NS pinching parameters ε_k of the edges E_k in B. The product is also over all vertices V_i and edges E_j in the graph Γ.

The analogous part of the bosonic string theory measure on Schottky space also takes a simple form in terms of the pinching parameters, obtained from Eq. (54) by deleting the $\mathrm{d}\Theta_i$'s and replacing $\mathrm{d}\varepsilon_j/\varepsilon_j^2 \mapsto \mathrm{d}k_j/k_j^2$ and $(1+q_B) \mapsto (1-k_B)$ [2].

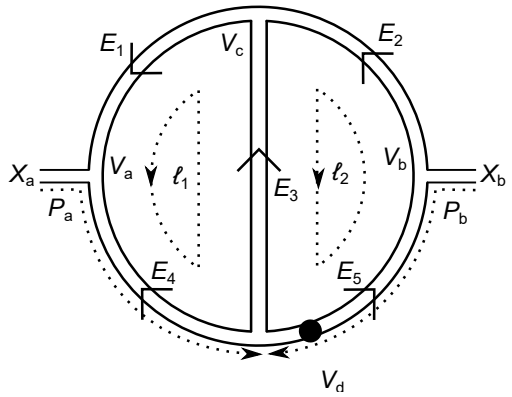

Figure 2: A directed cubic ribbon graph with $g = 2$, $n = 2$. Vertices are labelled V_i and internal edges have orientations marked by chevrons; the other labels have the same meanings as in Fig. 1.

4.2. Example

Consider the $g = 2$, $n = 2$ graph shown in Fig. 2. The loop basis indicated is given by

$$\ell_1 = \text{ACW}_d \cdot E_4^{-1} \cdot \text{CW}_a \cdot E_1 \cdot \text{CW}_c \cdot E_3 \cdot \text{ACW}_d \,, \tag{55}$$

$$\ell_2 = \text{CW}_d \cdot E_3^{-1} \cdot \text{CW}_c \cdot E_2 \cdot \text{CW}_b \cdot E_5 \,, \tag{56}$$

so with the dictionary Eq. (51) we find that the super Schottky group generators are

$$\boldsymbol{\gamma}_1 = \boldsymbol{\rho}_d \, \boldsymbol{\sigma}_4^{-1} \, \boldsymbol{\rho}_a^{-1} \, \boldsymbol{\sigma}_1 \, \boldsymbol{\rho}_c^{-1} \, \boldsymbol{\sigma}_3 \, \boldsymbol{\rho}_d \,, \tag{57}$$

$$\boldsymbol{\gamma}_2 = \boldsymbol{\rho}_d^{-1} \, \boldsymbol{\sigma}_3^{-1} \, \boldsymbol{\rho}_c^{-1} \, \boldsymbol{\sigma}_2 \, \boldsymbol{\rho}_b^{-1} \, \boldsymbol{\sigma}_5 \,. \tag{58}$$

Their semimultipliers are given by

$$q_1 = \varepsilon_1 \, \varepsilon_3 \, \varepsilon_4 \,, \qquad\qquad q_2 = \varepsilon_2 \, \varepsilon_3 \, \varepsilon_5 \,. \tag{59}$$

The fixed points are $\boldsymbol{u}_i = \frac{U_i^1}{U_i^2} \big| \frac{U_i^3}{U_i^2}$ and $\boldsymbol{v}_i = \frac{V_i^1}{V_i^2} \big| \frac{V_i^3}{V_i^2}$ where U_i and V_i are eigenvectors satisfying $\boldsymbol{\gamma}_i U_i = q_i^{-1} U_i$ and $\boldsymbol{\gamma}_i V_i = q_i V_i$, given by

$$U_1 = \boldsymbol{\rho}_d^{-1} \, \hat{U}_1 \,, \qquad V_1 = \boldsymbol{\rho}_d^{-1} \, \hat{V}_1 \,, \qquad U_2 = \hat{U}_2 \,, \qquad V_2 = \hat{V}_2 \,. \tag{60}$$

Here,

$$\hat{U}_i \equiv (1 - q_i^2\,,\, A_{I_i} \,|\, (1+q_i)\Phi_{I_i})^{\mathrm{t}}\,, \qquad\qquad \hat{V}_i \equiv (0\,,\, 1 \,|\, 0)^{\mathrm{t}} \tag{61}$$

where $I_1 = (4, 1, d, a, c)$, $I_2 = (3, 2, d, c, b)$ and

$$\Phi_{ij\alpha\beta\gamma} \equiv \Theta_\alpha + \varepsilon_i \Theta_\beta - \varepsilon_i \varepsilon_j \Theta_\gamma \tag{62}$$

$$A_{ij\alpha\beta\gamma} \equiv 1 + \varepsilon_i^2 + \varepsilon_i^2 \varepsilon_j^2 + \Theta_\alpha\, \Phi_{ij\alpha\beta\gamma} - \varepsilon_i^2 \varepsilon_j \Theta_\beta \Theta_\gamma. \tag{63}$$

Similarly, the paths from the external edges X_a, X_b to the marked base chart are given by

$$P_a = \textsc{acw}_d \cdot E_4^{-1} \cdot \textsc{cw}_a\,, \qquad\qquad P_b = E_5^{-1} \cdot \textsc{cw}_b\,, \tag{64}$$

then with Eq. (51) we find

$$\boldsymbol{V}_a = \boldsymbol{\rho}_d\, \boldsymbol{\sigma}_4^{-1}\, \boldsymbol{\rho}_a\,, \qquad\qquad \boldsymbol{V}_b = \boldsymbol{\sigma}_5^{-1}\, \boldsymbol{\rho}_b^{-1}\,, \tag{65}$$

so $\boldsymbol{x}_a = \infty|0$ and $\boldsymbol{x}_b = -\varepsilon_5^2| - \varepsilon_5 \Theta_b$. Let's instead use $\boldsymbol{V}_{a(\epsilon)}(z|\zeta) \equiv \boldsymbol{V}_a(z+\epsilon|\zeta)$ to control the infinities until we take $\epsilon \to 0$ in the final result. The three gauge-fixed points are $(\boldsymbol{a}, \boldsymbol{b}, \boldsymbol{c}) = (\boldsymbol{v}_1, \boldsymbol{v}_2, \boldsymbol{x}_{a(\epsilon)})$, so the super-projective volume element Eq. (53) is

$$\frac{1}{\mathrm{d}V_{\boldsymbol{v}_1 \boldsymbol{v}_2 \boldsymbol{x}_{a(\epsilon)}}} \sim \frac{1}{\epsilon\, \varepsilon_4^4} \frac{\mathrm{d}\Theta_{\boldsymbol{v}_1 \boldsymbol{v}_2 \boldsymbol{x}_{a(\epsilon)}}}{\mathrm{d}\boldsymbol{v}_1\, \mathrm{d}\boldsymbol{v}_2\, \mathrm{d}\boldsymbol{x}_{a(\epsilon)}}\,; \qquad\qquad \mathrm{d}\Theta_{\boldsymbol{v}_1 \boldsymbol{v}_2 \boldsymbol{x}_{a(\epsilon)}} \sim \mathrm{d}\Theta_d\,. \tag{66}$$

The denominators from the punctures are

$$(D\boldsymbol{V}_{a(\epsilon)}^{\zeta})(0|0) = \frac{1}{\epsilon\, \varepsilon_4}\,; \qquad\qquad (D\boldsymbol{V}_b^{\zeta})(0|0) = \varepsilon_5\,. \tag{67}$$

The super-Jacobian of the change from the canonical super Schottky variables to the pinching parameters is given in block form as $\left(\begin{smallmatrix} A & B \\ C & D \end{smallmatrix}\right)$ where

$$A = \frac{\partial(u_1, u_2, q_1, q_2, x_b)}{\partial(\varepsilon_1, \ldots, \varepsilon_5)} \qquad\qquad B = \frac{\partial(\theta_1, \theta_2, \xi_b, \Theta_{\boldsymbol{v}_1 \boldsymbol{v}_2 \boldsymbol{x}_{a(\epsilon)}})}{\partial(\varepsilon_1, \ldots, \varepsilon_5)} \tag{68}$$

$$C = \frac{\partial(u_1, u_2, q_1, q_2, x_b)}{\partial(\Theta_a, \ldots, \Theta_d)} \qquad\qquad D = \frac{\partial(\theta_1, \theta_2, \xi_b, \Theta_{\boldsymbol{v}_1 \boldsymbol{v}_2 \boldsymbol{x}_{a(\epsilon)}})}{\partial(\Theta_a, \ldots, \Theta_d)}\,; \tag{69}$$

its Berezinian is

$$\frac{\det(A - BD^{-1}C)}{\det D} = -8\frac{\varepsilon_3^2\varepsilon_4\varepsilon_5}{(1+q_1)(1+q_2)}(\boldsymbol{u}_1 \dot{-} \boldsymbol{v}_1)(\boldsymbol{u}_2 \dot{-} \boldsymbol{v}_2) \tag{70}$$

which combines with the other factors in the measure Eq. (52) to give

$$[\mathrm{d}\boldsymbol{m}_0]_2^2 = -8\,\mathrm{d}\Theta_a\,\mathrm{d}\Theta_b\,\mathrm{d}\Theta_c\,\mathrm{d}\Theta_d\,\frac{\mathrm{d}\varepsilon_1\,\mathrm{d}\varepsilon_2\,\mathrm{d}\varepsilon_3\,\mathrm{d}\varepsilon_4\,\mathrm{d}\varepsilon_5}{\varepsilon_1^2\,\varepsilon_2^2\,\varepsilon_3^2\,\varepsilon_4^2\,\varepsilon_5^2}(1+q_1)(1+q_2)\,. \tag{71}$$

This is of the form Eq. (54) because modulo conjugation ℓ_1 and ℓ_2 are the two closed boundaries of Fig. 2 (the closed path which crosses the edges $E_5E_2E_1E_4^{-1}$ is not a closed boundary because of the external edges X_a and X_b).

Acknowledgements

The authors would like to thank R. Russo and L. Magnea for useful comments and suggestions and collaboration on related projects. This work was supported by the Compagnia di San Paolo contract "MAST: Modern Applications of String Theory" `TO-Call3-2012-0088`.

Bibliography

[1] E. Witten, *Notes On Super Riemann Surfaces And Their Moduli*, `1209.2459`.

[2] S. Playle and S. Sciuto, "Pinching parameters for open (super) strings." In preparation.

[3] S. Mandelstam. *The Interacting String Picture and Functional Integration*, pp. 46–102 in M. B. Green *et al.*, eds., *Unified String Theories* (World Scientific, 1986).

[4] P. Dai and W. Siegel, *Worldline Green Functions for Arbitrary Feynman Diagrams*, *Nucl.Phys.* **B770** (2007) 107–122, [`hep-th/0608062`].

[5] P. Vanhove, *The physics and the mixed Hodge structure of Feynman integrals*, *Proc.Symp.Pure Math.* **88** (2014) 161–194, [`1401.6438`].

[6] P. Di Vecchia, L. Magnea, A. Lerda, R. Russo, and R. Marotta, *String techniques for the calculation of renormalization constants in field theory*, *Nucl.Phys.* **B469** (1996) 235–286, [`hep-th/9601143`].

[7] A. Frizzo, L. Magnea, and R. Russo, *Scalar field theory limits of bosonic string amplitudes*, *Nucl.Phys.* **B579** (2000) 379–410, [hep-th/9912183].

[8] E. J. Martinec, *Conformal Field Theory on a (Super)Riemann Surface*, *Nucl.Phys.* **B281** (1987) 157.

[9] Y. I. Manin. *Quantum Strings and Algebraic Curves*, pp. 1286–1295 in A. M. Gleason, ed., *Proceedings of the International Congress of Mathematicians, Berkeley, California, August 3–11, 1986* (American Mathematical Society, 1988).

[10] S. Playle, *Deforming super Riemann surfaces with gravitinos and super Schottky groups*, 1510.06749.

[11] L. Magnea, S. Playle, R. Russo, and S. Sciuto, *Multi-loop open string amplitudes and their field theory limit*, *JHEP* **1309** (2013) 081, [1305.6631].

[12] L. Magnea, S. Playle, R. Russo, and S. Sciuto, *Two-loop Yang-Mills diagrams from superstring amplitudes*, *JHEP* **1506** (2015) 146, [1503.05182].

[13] E. Witten, *Superstring Perturbation Theory Revisited*, 1209.5461.

[14] P. Di Vecchia, K. Hornfeck, M. Frau, A. Lerda, and S. Sciuto, *N-string, g-loop vertex for the fermionic string*, *Phys.Lett.* **B211** (1988) 301.